AIChE WILEY InterScience DISCOVER SOMETHING GREAT

ENVIRONMENTAL AND ENERGY ENGINEERING

# Drop Sizes during Turbulent Mixing of Toluene–Heavy Oil Fractions in Water

**Chandra W. Angle and Hassan A. Hamza**
Natural Resources Canada, CANMET Energy Technology Centre, Devon, Alberta, Canada T9G 1A8

*DOI 10.1002/aic.10862*
*Published online April 11, 2006 in Wiley InterScience (www.interscience.wiley.com).*

*The properties of heavy oil emulsions produced in heavy oil extractions processes often fluctuate, thus making treatments difficult. We investigated whether oil-phase ratios and flow conditions might influence these emulsions. We studied turbulent mixing effects on droplet sizes in real time, using a fully baffled stirred tank with a Rushton turbine in bench-scale batch experiments. Breakup/coalescence of various volume fractions of toluene diluted heavy oil in model process water was measured at four mixing speeds. The range of oil volume fractions was 0.01 to 0.3, where 0.01 is the Kolmogorov limit and 0.3 the upper limit for oil-in-water (O/W) emulsions. Results showed that size distributions depended on mixing time, rpm, and oil fractions. Breakage dominated at low oil fraction 0.01 and high mixing intensities produced bimodal distributions. The persistence of finer droplets was attributed to reduced coalescence. Steady state was not reached. The middle range oil fractions (0.05, 0.1) approached steady state more quickly and followed a first-order breakage model at 800 rpm. The size distributions narrowed before the end of the mixing time. The highest oil fractions and lowest mixing speeds produced the largest droplet sizes. Plots of $d_{32}$ vs. rpm for 75 min mixing showed that as the volume fraction of oil phase increased the shapes of the curves changed from concave to linear to convex. The $d_{32}$ vs. energy dissipation curves suggested that turbulent dampening reduced breakage. However, drop coalescence from erosive collisions as well as droplet surface elasticity were factors affecting droplet sizes.*
*AIChE J,* 52: 2639–2650, 2006
*Keywords: heavy oil, droplets, breakage, coalescence, size distributions, turbulent, stirred tank*

## Introduction

Heavy oil emulsions are produced during extractions from deep wells and reservoirs. The characteristics and properties of these emulsions vary on a daily basis and are often difficult to treat. The formation and stability of these emulsions are still not understood.[1] During extraction the oils are mixed with process water and sand as they flow, mostly turbulently, through the pipes. Thus understanding of the droplets' formation and stability during turbulent flow is necessary for prescribing treatments of produced water before discharge into the environment, and for heavy oil recovery.

Turbulent agitation of increased dispersed-phase volume fractions (holdup) of clean model oils without surfactants in water produces increased droplet sizes.[2-4] This response has been explained as an effect of *turbulence dampening*,[5] which means the death of low-energy smaller eddies in flow and the survival of the high-energy larger eddies. During turbulent agitation of increased dispersed-phase holdup in a fixed tank volume, a high number density of droplets is produced and collision frequency can be expected to increase. Without surface-active barriers at the interface, droplets of clean model oil

Correspondence concerning this article should be addressed to C. W. Angle at angle@nrcan.gc.ca.

readily coalesce on collision when the collision time is greater than the film drainage time.[6-8] Heavy oils contain natural surfactants that migrate to the oil/water interface of droplets. Toluene-diluted heavy oils with the self-contained surfactants and stabilizers are expected to behave differently from model oils. Coalescence time is expected to be longer than collision time. Such studies on stability effects for increased holdup of dispersed heavy oil phase, during turbulent agitation in a stirred tank, have not been explored or found in the open literature to date.

Our earlier results indicated that droplets of various heavy oil concentrations in toluene responded differently to reduction in turbulence intensity compared to surfactant-free model toluene.[9] We showed that at a fixed oil fraction ($\Phi = 0.05$) in water, the heavy oil droplets for 25 wt % heavy oil in toluene had a layer of adsorbed stabilizers at the oil/water interface and were more stable to breakage and coalescence (at 800 rpm: Reynolds number 34,400) than droplets with lesser surface coverage. We also showed in another three-phase (oil–water–sand) mixing study that increased shearing of the 25 wt % heavy oil-in-toluene droplets in the presence of sand caused a significant increase in droplet breakage.[10,11] Thus it is expected that during turbulent mixing of two phases, by varying energy dissipation levels and/or volume fractions of this 25 wt % heavy oil, the breakage and coalescence behavior of the droplets in the same water would respond unlike the extensively studied model oils.[1,12,13] The adsorbed films of interfacially active asphaltenes and resins[14] inside the droplets at the oil/water interface can lead to different droplet responses for increased intensities of turbulent flow. During turbulent agitation, it is expected that coalescence time will be longer than collision time,[15] thereby affecting the resulting transient size distributions.

To our knowledge, studies on the effects of increased volume fractions of dispersed heavy oil phase, during turbulent agitation, have not been published to date in the open literature.[11] Thus the objectives of this study are to measure the transient droplet size distributions of the heavy oil droplets formed for varied turbulent intensities and oil fractions and to gain some insight into the emulsion stability under these conditions.

The present article investigates the effects of varied volume fractions of a 25 wt % heavy oil in toluene during turbulent mixing in model process water. The stability of the oil-in-water emulsion systems is monitored while varying the mixing rpm of a Rushton turbine for fixed oil fractions, and while varying oil fractions at fixed rpm. Droplet size distributions and Sauter mean diameters ($d_{32}$) are measured as a function of time during continuous agitation and after rest. The $d_{32}$ data are collected in real time for heavy oil droplets produced at four impeller speeds for four volume fractions of dispersed phase.

## Experimental

### Materials

Heavy oil from a steam-assisted gravity drainage process (SAGD) in Primrose Alberta was used in this study. The concentrations of the groups of chemical structures that make up the solubility classes (SARA) in this oil were: saturates (S) 23 wt %, aromatics (A) 21.1 wt %, resins (R) 38.8 wt %, and asphaltenes (A) 17.1 wt %. The average molecular weight was 534 g/mol,[16] density at 22°C was 1003 kg/m$^3$, viscosity at 24°C was >10,000 mPa·s, and American Petroleum Institute gravity degrees (°API gravity) was 10–11. The simulated process water ($mpH_2O$), as previously described,[10] was a mixture of 0.01 mol/L $NaHCO_3$, $1.8 \times 10^{-6}$ mol/L $CaCl_2$, and $1.37 \times 10^{-4}$ mol/L $K_2CO_3$ in deionized water prepared from Millipore reverse osmosis and Milli-Q polishing. The pH of $mpH_2O$ was 8.5 and specific conductivity around 870 $\mu$S/cm. All salts were 99.9% purity Sigma grade from Aldrich Chemicals. The HCl and NaOH were ACS grade, whereas toluene was a spectroscopic grade from Fisher Scientific. All buffers and conductivity standards were obtained from Fisher Scientific.

**Table 1. Experimental Conditions and Fluid Properties at 22°C**

| Experimental Conditions | |
|---|---|
| Mixing time, min | 100 |
| Sampling times, min | 1, 8, 15, 25, 35, 45, 60, 75, 90, 100 |
| Impeller speeds, rpm | 600, 700, 800, and 900 |
| Reynolds number range | 25,800 to 38,700 |
| Weber numbers | 657, 895, 1169, and 1479 |
| Impeller diameter, $D$, cm | 5.08 |
| Tank diameter, $D_T$, cm | 10.43 |
| Power number, $P_0$ | 5.1 ± 0.3 |
| Off-bottom clearance, $D_T/3$, cm | 3.47 |
| **Fluid Properties** | |
| Volume fractions of oil | 0.01, 0.05, 0.1, 0.3 |
| Wt % heavy oil in toluene | 25 |
| O/W interfacial tension, mN/m | 19.9 |
| Dilatational elasticity at 50 Hz, mN/m | 4.8 |
| Viscosity of oil, mPa · s | 1.56 |
| Density of oil, kg/m$^3$ | 895.45 |
| Asphaltenes in oil, wt % | 4.28 |
| Density of $mpH_2O$, kg/m$^3$ | 998.3 |
| Viscosity of $mpH_2O$, mPa · s | 1.00 |
| pH of $mpH_2O$ | 8.5 |

A Malvern Mastersizer 2000 laser light scattering instrument and the HydroSM small-volume recirculating cell were used for size analysis. Oil viscosity was measured using the Ubbelohde capillary viscometer. All samples were equilibrated at controlled-temperature baths at 22°C. Densities were measured at 22°C with a Paar DMA 4500 densitometer by direct injection. Details of the mixing apparatus are published elsewhere.[9,11]

### Methods

*Sample Preparation.* The 25 wt % heavy oil in toluene was prepared by weighing 25 g oil into a graduated glass jar containing preweighed toluene (75 g). The mixture was shaken for 2 h using a horizontal shaker until no lumps were seen under the microscope at 100 × magnification. The physical properties of the toluene-diluted heavy oil (from hereon referred to as "the oil"), are shown in Table 1. The selected concentration of 25 wt % heavy oil in toluene was previously shown to produce stable emulsions at an oil volume fraction of 0.05 and 800 rpm.[9]

*Mixing and Sampling.* The experimental procedures closely followed those of our earlier reported studies, which showed details of the mixing apparatus, sampling, and droplet detection.[9-11] In the experiments herein, kinematic, dynamic,

and geometric similarities to conventional larger-scale stirred tank systems were maintained. Mixing was conducted as a batch process in a 1-L flat-bottom cylindrical glass tank of diameter $D_T = 10.43$ cm and with liquid height $H$ equal to tank diameter $D_T$. The diameter of the Rushton impeller was $D_T/2$. The impeller height was at off-bottom clearance of $D_T/3$. There were six baffles symmetrically spaced in the tank. The Rushton impeller speeds were controlled in time with a Lightnin mixer-motor. All the systems were preconditioned with the water phase before the start of mixing. A volume fraction of stock-diluted heavy oil was layered over the water in the mixing tank for a period of 1–1.5 h of preequilibration before the start of mixing. The fraction of the conditioned oils was mixed in model process water for 100 min at specified speed (rpm). Mixing was not interrupted during sampling. Samples were aspirated using a positive-displacement syringe attached to a Teflon® capillary. The latter was inserted at the level of impeller offshoot in the tank. In one continuous motion the emulsion was sampled and deposited into the HydroSM sampler of the Mastersizer in $<10$ s. The details of fluid properties, mixing conditions, tank dimensions, and sampling times are summarized in Table 1.

In the present study, the highest volume fraction of oil is $\Phi_{oil} = 0.3$, which is the limit for dispersed oil in water.[4] Agitation speeds are listed in Table 1. Visible air entrainment began at 1000 rpm; therefore all mixing was kept below this speed. Timing began from the start of mixing at a fixed speed and samples were removed for droplet size distribution analysis after 1, 8, 15, 25, 35, 45, 60, 75, 90, and 100 min of continuous agitation. Emulsion samples were removed as mixing continued. Sets of 16 experiments in a matrix of four mixing speeds and four volume fractions were conducted. Numbers of samples analyzed per set were $4 \times 4 \times 10$ as volume fraction, mixing speeds, and time varied, respectively. Duplicate sets were measured to confirm the observations. The Sauter mean diameter $d_{32}$ and size distributions of droplets were measured by light scattering methods using the Mastersizer 2000. Both sampling and size distribution measurement[9] were completed typically within 20 s. Size distributions were again measured after 24 h of rest.

## Results and Discussion

The following results are presented for fixed volume fractions of oil at varied agitation speeds, followed by comparative graphs for fixed speeds at four oil fractions. The results are discussed in relation to our previously published studies with concomitant explanations published by others on behaviors of model systems during stirred tank mixing.

### *Size distributions and $d_{32}$ vs. time for fixed $\Phi_{oil}$ at four agitation speeds*

Figures 1 to 4 show plots of $d_{32}$ vs. agitation time for droplets from oil volume fractions 0.01, 0.05, 0.1, and 0.3, at mixing speeds of 600, 700, 800, and 900 rpm, respectively. Following each of these plots are drop size distributions in Figures 1b–1g, 2b–2e, 3b–3e, and 4b–4e for emulsions formed at selected times of agitation between 1 and 100 min. The experimental size distributions fitted lognormal distribution functions at $R^2$ of 98% or better for all tested volume fractions of oil. The size distributions for times not shown are the transients. Some selected size distributions of 24-h aged creamed emulsions are also shown in Figures 1e and 1g to illustrate emulsion stability.

At the lowest oil fraction at $\Phi_{oil} = 0.01$ (well within theoretical boundaries for applying breakage arguments according to Hinze–Kolmogorov theory[12,17]), there are wide differences between $d_{32}$ values for 600 and 900 rpm, and some fluctuations in droplet size were initially observed for the 600 rpm mixing speed. As expected, the droplet sizes were the largest at 600 rpm. At 600 rpm, for which one expects the lowest intensity of turbulence—and thus low kinetic energy—the large sizes are often interpreted as being attributed to lessened droplet breakage arising from the larger turbulent eddies in the fluid. The 700 rpm curve coincided with the 800 rpm curve up to 60 min, after which the latter showed a stepped drop in $d_{32}$, whereas the former decreased at the same rate. At 800 rpm the droplet size reduction coincided with that for 900 rpm for 15 min, decreased at steady rate for 60 min, then showed a stepped decrease in size. After 75 min, the size reduction rate did not change up to 100 min of mixing. At 900 rpm, within 35 min a temporary plateau in droplet size was reached. After 35 min, a stepped decrease in $d_{32}$ is shown with mixing time. Droplet size steadily decreased up to 100 min mixing. These behaviors were found repeatable. The size distributions for $\Phi_{oil} = 0.01$ are shown in Figures 1b to 1g. A secondary peak of finer particles appears at the time when $d_{32}$ underwent a marked decrease (see Figures 1d–1g). The bimodal size distributions for heavy oil volume fractions of 0.01 at 800 and 900 rpm reflect the step change in average droplet size.

The observed stepped change in droplet sizes can be explained by analogy to the two steady-state sizes that Kumar et al.[18] presented in their multistage breakage model for drops under turbulent flow. Their model treats a drop as a Voigt element with deformation and relaxation occurring in stages after several passes from impeller to tank. Breakage occurs after the strain becomes unity. The drop recovery after deformation is dependent on the relative restoring stresses of interfacial tension and the viscous resistance to deformation. According to these authors, full recovery does not always occur, and so the strain may approach unity as turbulent intensity and mixing time increase. Thus, complete breakup occurs in stages with mixing time.

Secondary drop sizes are not unusual in industrial processes. Desnoyer et al.[19] explained the phenomenon as the breakage of one drop into two daughter drops and "satellite" droplets as a result of stretching of a liquid filament just before the daughter drops separate. The thin filament undergoes breakup by Rayleigh instabilities.[20] Baldyga et al.[21] used an extended theory of drop breakup by suggesting turbulence intermittency to explain the drift toward smaller drops as agitation is maintained. However, erosive breakage by shear stresses of fluids flowing tangentially off the impeller blades should not be ruled out at low oil fractions. In water, the low dispersed phase volume fraction of 0.01 (for 25 wt % heavy oil in toluene) and high turbulence intensity support reduced coalescence, after breakage by elongation stresses. Pacek et al.[22] observed bimodal size distributions with turbulent mixing at low speeds for $<5\%$ chlorobenzene in deionized water. However, they found that, at higher fraction of dispersed phase, the bimodality diminished. It is not unusual to find these unwanted finer droplets, which are seen as a "haze," in turbulent mixing of very dilute indus-

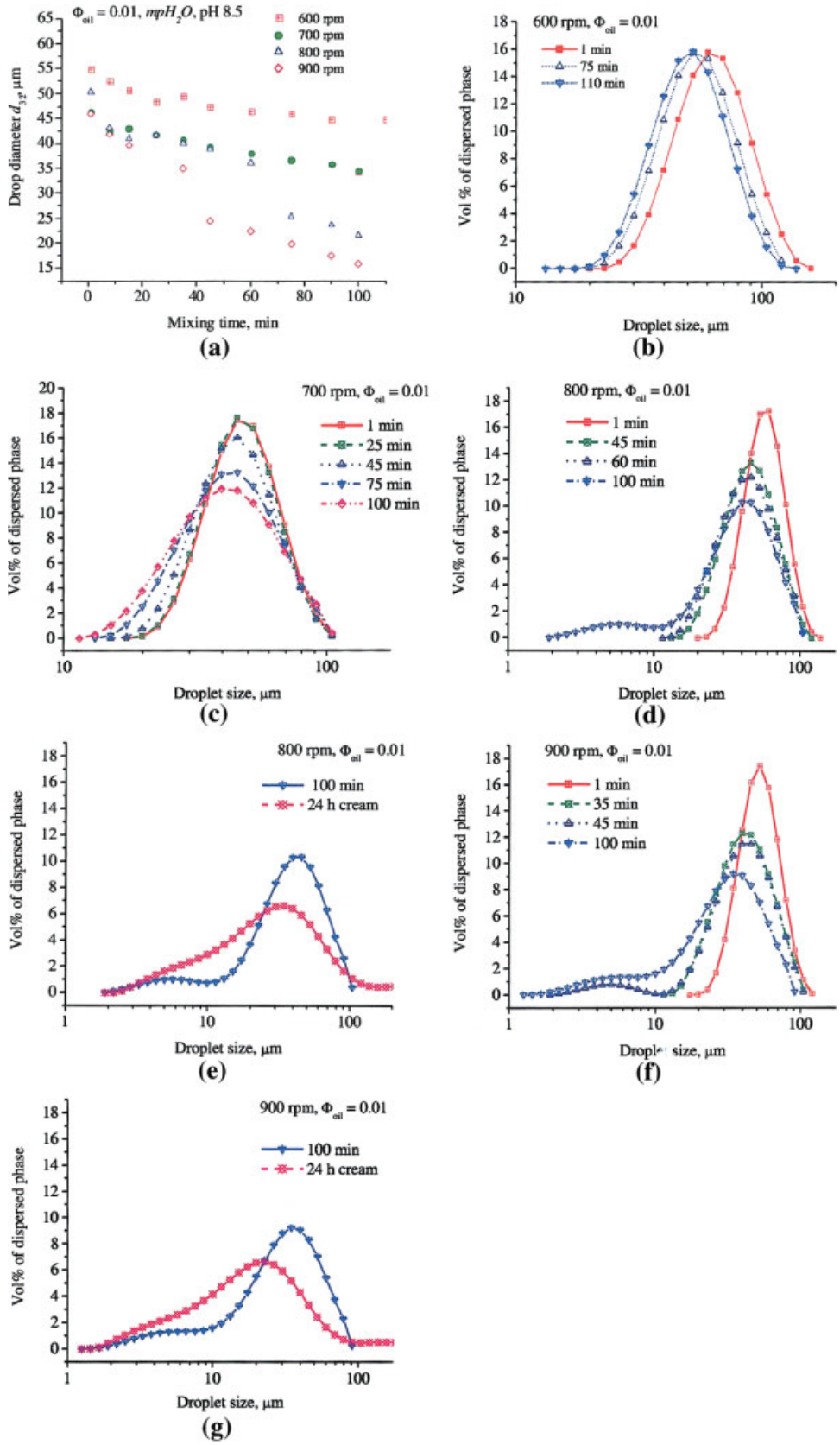


**Figure 1. (a) Decrease in diameters of oil droplets for $\Phi_{oil}$ = 0.01 in model process water ($mpH_2O$) as a function of agitation times and impeller speeds of 600 to 900 rpm. Size distributions of oil droplets in water for $\Phi_{oil}$ = 0.01 measured for various times at (b) 600 rpm, (c) 700 rpm, (d) 800 rpm, (e) 800 rpm (at 100 min and after 24 h of rest), (f) 900 rpm, and (g) 900 rpm (at 100 min and after 24 h rest).**

[Color figure can be viewed in the online issue, which is available at www.interscience.wiley.com]

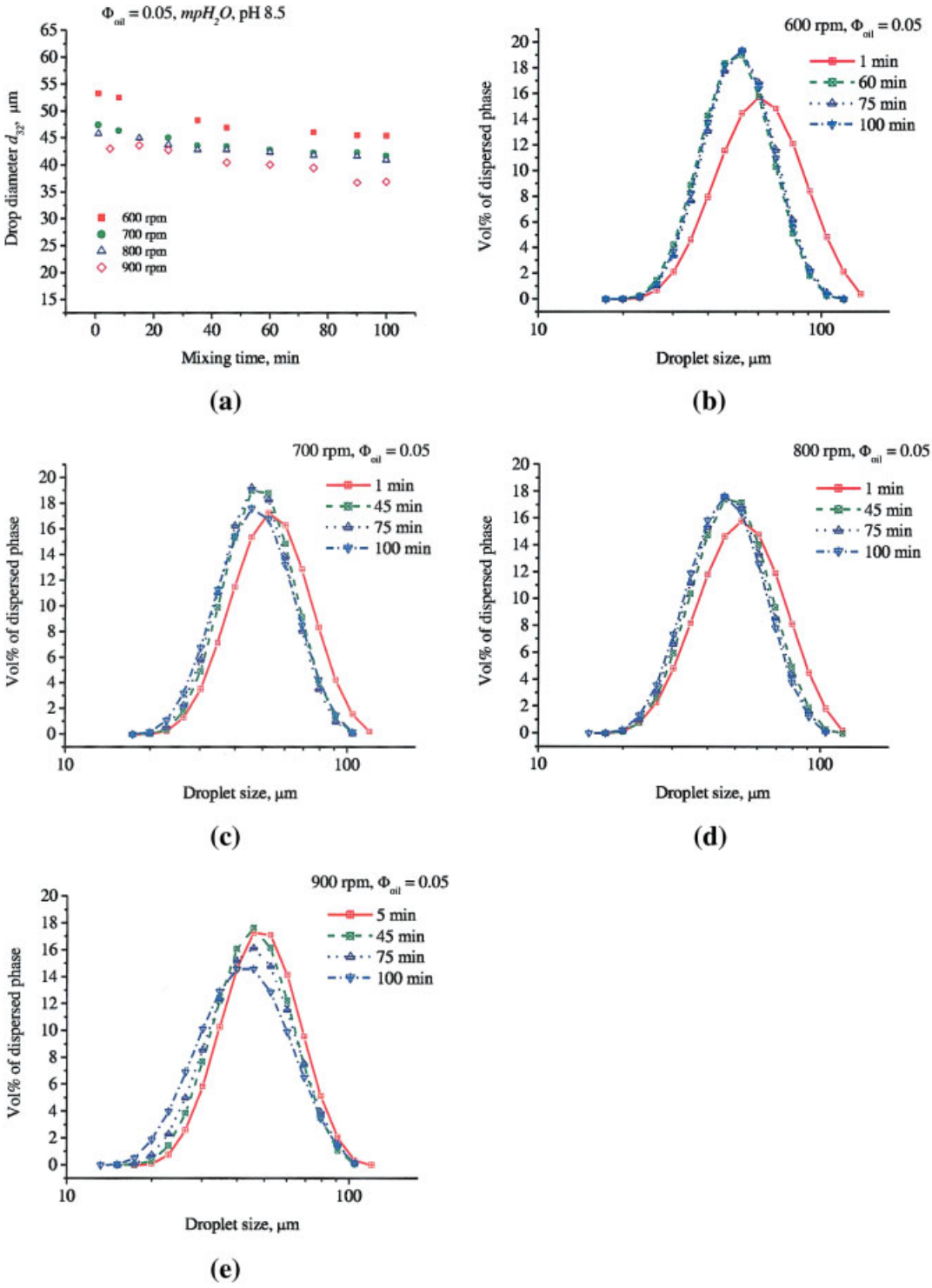


**Figure 2. (a) Decrease in diameters of oil droplets for $\Phi_{oil} = 0.05$ in model process water ($mpH_2O$) as a function of agitation times and various impeller speeds. Size distributions of oil droplets in water for $\Phi_{oil} = 0.05$ measured for various times at (b) 600 rpm, (c) 700 rpm, (d) 800 rpm, and (e) 900 rpm.**

[Color figure can be viewed in the online issue, which is available at www.interscience.wiley.com]

trial systems.[4] It appears that the bimodal droplet sizes observed in this present work can be well explained by these arguments, even though our drop viscosity is small.

For breakage, generally the dynamic interfacial properties, viscosity ratios of dispersed to continuous phases, and flow conditions are significant factors. Because the present diluted heavy-oil system has a viscosity $< 10$ mPa·s, which is the limit above which viscous resistance is significant, the resistance to

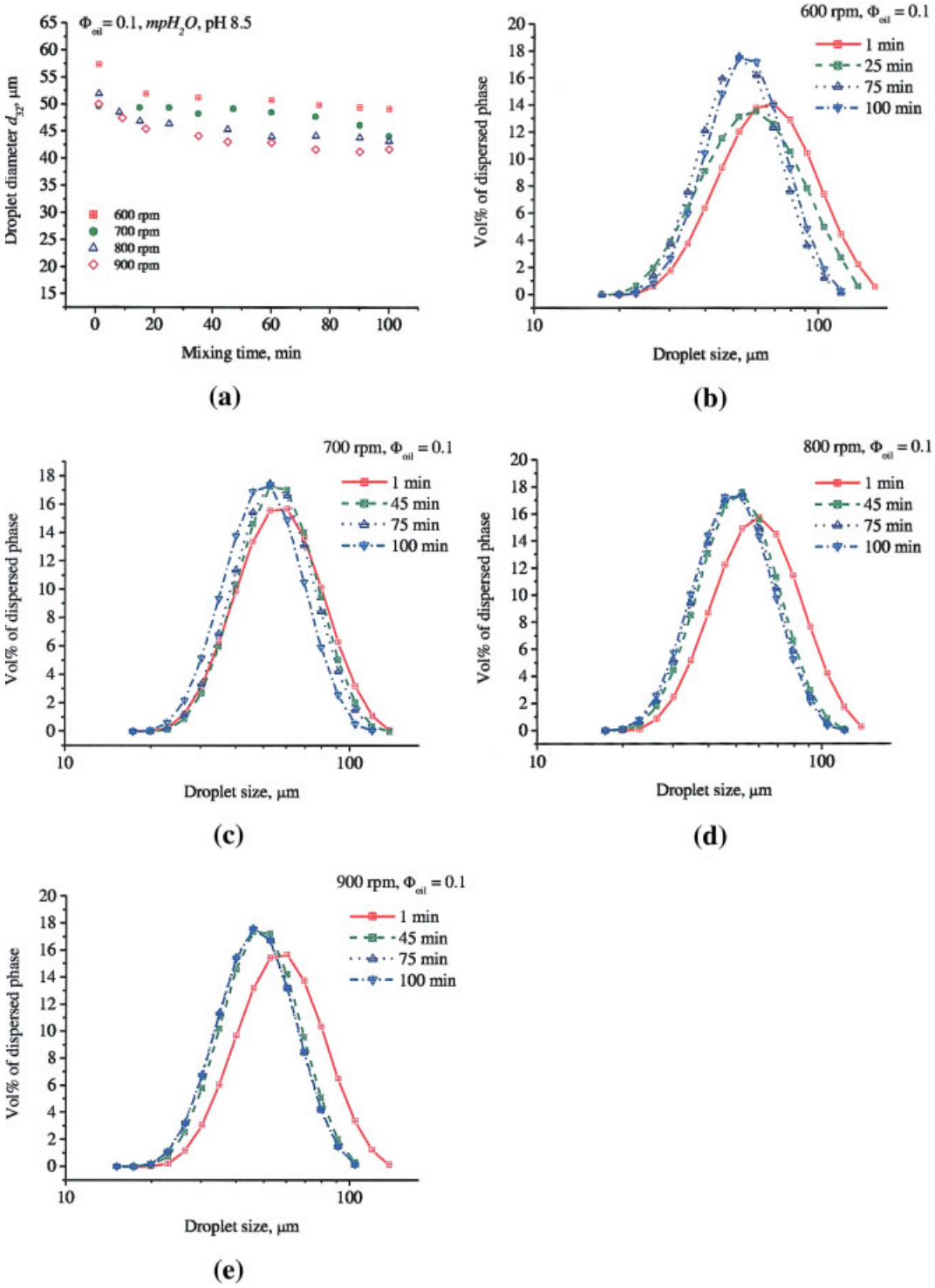


**Figure 3. (a) Decrease in diameters of oil droplets for $\Phi_{oil}$ = 0.01 in model process water ($mpH_2O$) as a function of agitation times and various impeller speeds. Size distributions of oil droplets in water for $\Phi_{oil}$ = 0.1 measured for various times at (b) 600 rpm, (c) 700 rpm, (d) 800 rpm, and (e) 900 rpm.**

[Color figure can be viewed in the online issue, which is available at www.interscience.wiley.com]

breakage for the initial period at 800 and 900 rpm might be attributable to viscoelasticity in the drop, as discussed in our earlier work.[9,11] A buildup of a thick adsorbed layer of surface-active film (40–60 nm for 40 Pa and 21.4 nm at 135 Pa pressures for mass ratio 1:3 of bitumen:toluene) was reported.[14] This is by analogy comparable to film inside the droplets in our case for the 25 wt % oil-in-toluene system. We showed that the viscosity of oil-in-toluene systems increases dramatically at

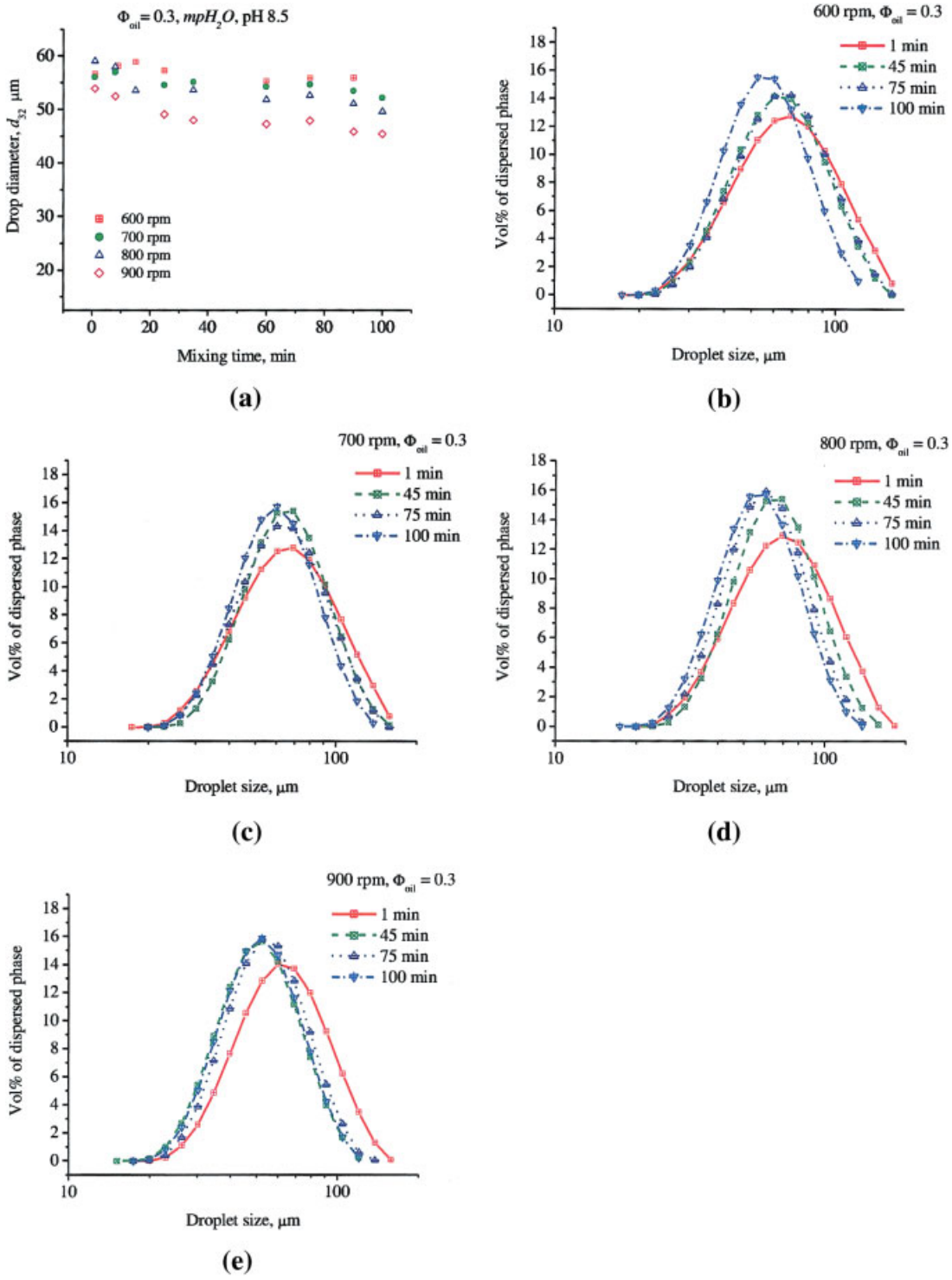


**Figure 4. (a) Changes in diameters of oil droplets for $\Phi_{oil}$ = 0.3 in model process water ($mpH_2O$) as a function of agitation times and various impeller speeds. Size distributions of oil droplets in water for $\Phi_{oil}$ = 0.3 measured for various times at (b) 600 rpm, (c) 700 rpm, (d) 800 rpm, and (e) 900 rpm.**

[Color figure can be viewed in the online issue, which is available at www.interscience.wiley.com]

around 25 wt % (still <10 mPa·s).[23] This indicated that viscosity was too high for achieving a steady-state interfacial tension during droplet deformation and/or the asphaltenes may be self-associating inside the heavy oil droplets. These interactions, which lead to the rise in viscosity similar to that of macromolecules, may also oppose oil droplet breakage from elongation stresses. Koshy et al.[24] showed that, subject to the same turbulence, viscoelastic drops tend to be larger than

inviscid drops. Similarly, Walter and Blanch[25] gave an explanation of interfacial elasticity as being responsible for the persistence of large droplets of air bubbles coated with high molecular weight surfactants.

Te 24-h aged samples in sealed microscope slides maintained the integrity of most of the droplet population, especially the finer sizes, even though they were closely packed in the slide. This indicated that a protective barrier kept the droplets stable on standing. Our visual observations were that creamed emulsions, which were exposed to air over time, broke in the jar, thus eliminating some larger droplets in the aged samples from the jars.

It appeared that breakup of droplets continued over the experimental time for an oil-phase ratio 0.01 and no steady state was reached within the time frame for measurements. At this lower oil-phase ratio 0.01, reduced collision frequency favors breakage over coalescence. Agitation at 600 or 700 rpm over time did not supply sufficient turbulence intensity for further breakage, and eddy time was less than drop relaxation time. However, agitation at 800 and 900 rpm did, and resulted in secondary peaks in the droplet size distributions and decreased droplet sizes.

For $\Phi_{oil} = 0.05$ (Figure 2), 0.1 (Figure 3), and 0.3 (Figure 4) at the four mixing speeds, the $d_{32}$ vs. time curves segregated into groups as oil volume fraction increased. Figure 2 shows that the 600 rpm curves for $\Phi_{oil} = 0.05$ still have the largest droplets with agitation time, whereas the 700 and 800 rpm curves coincided and separated from the 900 rpm curve after 45 min of mixing. From 700 to 900 rpm, the gap between $d_{32}$ values at equal time intervals for each volume fraction of heavy oil narrowed as the volume fraction increased. The 700 rpm run for $\Phi_{oil} = 0.1$ (Figure 3) approached the 600 rpm run, and for $\Phi_{oil} = 0.3$ (Figure 4) the 600, 700, and 800 rpm runs were separated from the 900 rpm run. Steady state, shown by leveling of size vs. time curve, was reached quickly and was maintained at oil volume fractions 0.05 to 0.3. There were no secondary droplets or tails observed at the higher oil volume fractions in the agitated vessel, which is consistent with observations of Pacek et al.[22] on model systems.

As agitation time progressed for each $\Phi_{oil} > 0.01$, the size distributions narrowed and reached a near steady state before the end of the mixing at 100 min. The exception for $\Phi_{oil} = 0.05$ is at 900 rpm (Figure 2e), when the 100 min distribution shifted to smaller sizes than the 75 min distribution. For $\Phi_{oil} = 0.1$ (Figures 3b–3e), this shift in distributions occurred only at 700 rpm for the 100 min sample. For 800 and 900 rpm, the size distributions in each run were superimposed after 45 min of mixing. At $\Phi_{oil} = 0.3$ (Figures 4b–4e), the 600 rpm distributions were more broadened initially to 75 min and at 100 min became narrower. This pattern was consistent for distributions measured for 700, 800, and 900 rpm, as well.

### *Effects of oil-phase volume fractions on droplet size distribution*

The $d_{32}$ vs. time curves for various volume fractions and fixed impeller speeds are compared in Figures 5 to 8. At 600 rpm, there were minor differences between the $d_{32}$ vs. time curves for $\Phi = 0.01$ and 0.05, and some differentiation between $\Phi = 0.1$ and 0.3 curves. The gaps between the $d_{32}$ vs. time curves at the four volume fractions were widest at 700 rpm (Figure 6). However, at 800 rpm, values of $d_{32}$ vs. time for volume fractions of 0.1 and 0.05 were closer together and were separated from the curves for $\Phi_{oil} = 0.3$ on one side and $\Phi_{oil} = 0.01$ on the other. At 900 rpm the $d_{32}$ vs. time curve for $\Phi_{oil} = 0.01$ deviated from the curves for $\Phi = 0.05$ and 0.1, which again were closer to the $d_{32}$ vs. time curve for $\Phi_{oil} = 0.3$.

The increase of droplet size with increased $\Phi_{oil}$ is consistent with published data on model oils. For turbulently agitated model oils with and without stabilizers droplet sizes increased at high volume fractions of the oil-dispersed phase.[5,19,26-29] The behavior was generally attributed to coalescence by a higher collision frequency between droplets.[15,30-32]

The droplet sizes of our systems with higher $\Phi_{oil}$ quickly reached steady state. They appeared to show less breakage with time (slope of $d_{32}$ vs. agitation time curve) for $\Phi_{oil} \geq 0.05$, even at higher agitation speeds. This suggests droplet death rate

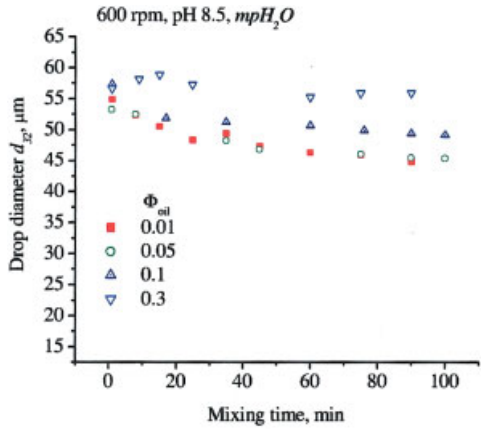


**Figure 5. Changes in diameters of oil droplets formed in model process water (*mpH$_2$O*) as a function of agitation time at 600 rpm for $\Phi_{oil}$ = 0.01, 0.05, 0.1, and 0.3.**

[Color figure can be viewed in the online issue, which is available at www.interscience.wiley.com]

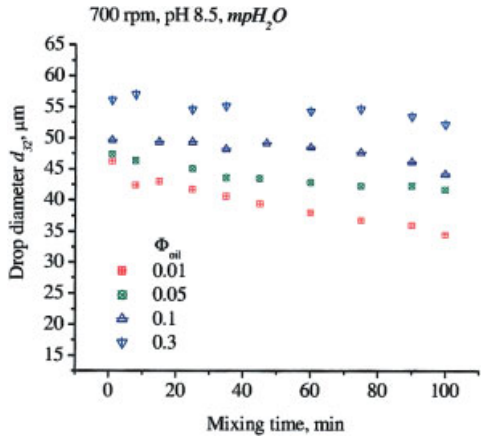


**Figure 6. Changes in diameters of heavy oil droplets formed in model process water (*mpH$_2$O*) as a function of agitation times at 700 rpm for $\Phi_{oil}$ = 0.01, 0.05, 0.1, and 0.3.**

[Color figure can be viewed in the online issue, which is available at www.interscience.wiley.com]

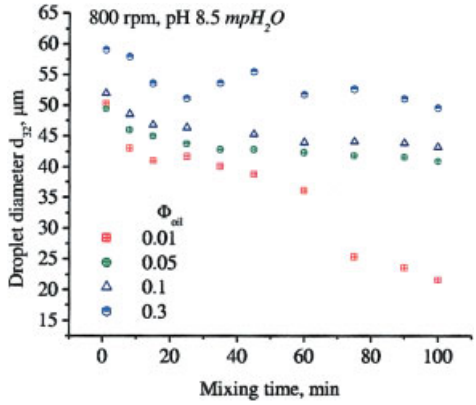


**Figure 7. Changes in diameters of heavy oil droplets formed in model process water ($mpH_2O$) as a function of agitation time at 800 rpm for $\Phi_{oil}$ = 0.01, 0.05, 0.1, and 0.3.**

[Color figure can be viewed in the online issue, which is available at www.interscience.wiley.com]

(breakage into smaller droplets and coalescence to larger droplets) equals birth rates (breakage of larger droplets and coalescence of smaller droplets).[33] The results indicate that the turbulent energy effect was significant in droplet breakage, but only until steady state was reached. Breakage probability can be a function of droplet sizes as well.

The conventionally accepted explanations for this behavior, in contactor studies, are that the increased number density of droplets increases the probability of collisions, thus leading to increased drop–drop coalescence. The increased volume fraction of oil dampens the turbulent eddies, leaving the eddy lengths much larger than droplet diameters. As a result, the droplets cannot be broken further.[4] Turbulent dampening at large dispersed phase ratio is used frequently as an explanation for larger droplet sizes.[5] As the particle number density grows high, however, coalescence takes place only if interfacial film thinning occurs before the intrusion of a turbulent eddy. The film drainage time should be less than the collision time for coalescence to occur.[34] If the droplet does not recover from deformation because of a relatively immobile film, it is partially on the way of a dimple formation in film drainage mechanism when contact is made with another dimpled droplet. Breakage, on the other hand, will occur only after many passes from impeller to tank for these systems.

The argument for reduced coalescence for this oil concentration in toluene relative to others at a volume fraction of 0.05 was presented in an earlier study.[9] A stepped reduction in agitation speed then did not change the droplet sizes. This resistance to coalescence was attributed to the larger film thickness and reduced film elasticity that prohibit immediate coalescence on drop–drop contact in the less-intense turbulent flow. Interfacial elasticity of asphaltene films for crude oil-in-water emulsions has been measured[35] in the range of 0.12 to 0.74 mN/m and up to 2 mN/m for crude oils.[36] For the system under study interfacial dilatational elasticities from 4.8 to 10.1 mN/m at oscillation frequencies from 50 to 5 Hz were measured using pendant drop oscillation. On the other hand, coalescence in a "rest" situation when film drainage is the controlling event is treated as a series of intricate phenomena that are dependent on the mobility of interfaces, internal phase viscosity, interfacial tension gradients, fluid circulation within the phases, velocity of approaching interfaces of two drops, and squeezing flow properties of fluids in the lamellae.[1,37] In turbulent flow coalescence events are treated statistically with respect to drop breakup and drop collisions.

Increasing the speed of collisions would enhance coalescence because deformation on collision will bring bare patches on the droplet surfaces. Sovova[30] attributed coalescence in high dispersed-phase holdup to erosive collisions, which favor coalescence as a result of contacting of bare patches on the surface of droplets. We pursue this point further in another study by using a stator-rotor to homogenize oil droplets at increased heavy oil fractions.[11]

A more detailed view of the droplet breakage processes at increased dispersed oil phase ratios can be seen in the size distributions at fixed times of agitation (Figures 1b–1g to 4b–4e). Even after 24 h, the droplets persisted, although the smaller droplets survived the larger ones, as shown in the measured distributions. However, our recorded video images showed that the droplets were stable if undisturbed over 24 h and broke only if exposed to air. Drainage of lamellae toward coalescence was a very slow process on standing.

Figure 9 shows a summary of $d_{32}$ vs. impeller speeds for the four volume fractions of oil after 75 min of mixing. The shapes of the $d_{32}$ vs. rpm curves for increased volume fractions changed from concave ($\Phi_{oil}$ = 0.1) to linear ($\Phi_{oil}$ = 0.05 and 0.1) to convex ($\Phi_{oil}$ = 0.3). These are of practical interest because the droplets from oils at $\Phi_{oil}$ = 0.05 and 0.1 behave similarly compared to $\Phi_{oil}$ = 0.3, which shows the beginning of change toward inversion and lessened stability. However, from a theoretical perspective, comparisons based on energy dissipation below are more informative.[38] The responses are shown next under equivalent energy dissipation. The results of the studies at higher oil fractions are reported in another study under the topic phase inversion.[11]

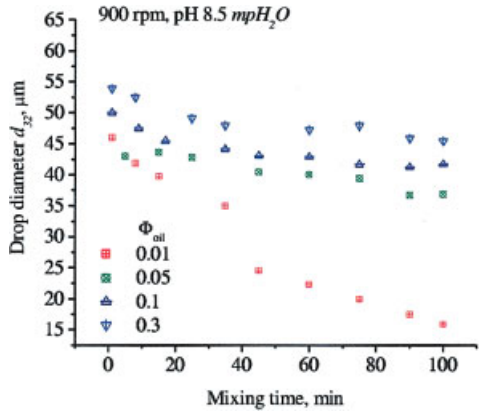


**Figure 8. Changes in diameters of heavy oil droplets formed in model process water ($mpH_2O$) as a function of agitation time at 900 rpm for $\Phi_{oil}$ = 0.01, 0.05, 0.1, and 0.3.**

[Color figure can be viewed in the online issue, which is available at www.interscience.wiley.com]

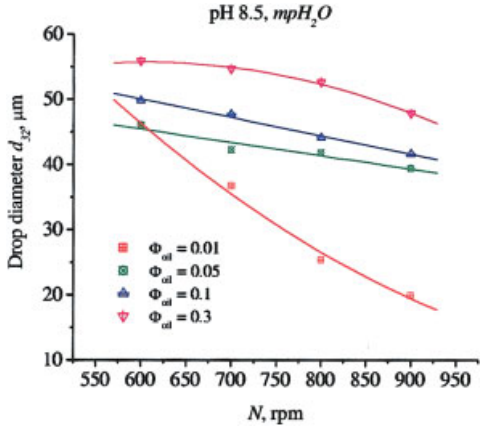


**Figure 9. Summary of $d_{32}$ vs. impeller speeds for various oil fractions at 75 min of mixing.[38]**

[Color figure can be viewed in the online issue, which is available at www.interscience.wiley.com]

### *Comparing the $d_{32}$ vs. average energy dissipation $\bar{\varepsilon}_T$ at increasing volume fractions of oil phase*

Figure 10 shows the droplet diameter vs. average energy dissipated in the tank $\bar{\varepsilon}_T$ for the four volume fractions of dispersed oil phase. The $d_{32}$ values are those measured after 75 min of agitation. The experimental $d_{32}$ values for $\Phi_{oil}$ = 0.01 and 0.05 are almost the same at the same energy dissipation (2.2 W kg$^{-1}$). Above 2.2 W kg$^{-1}$, a differentiation in size at equal energy input is shown. The decrease in size with increase in $\bar{\varepsilon}_T$ was greatest for the lowest volume fraction (that is, $\Phi_{oil}$ = 0.01), confirming that breakage was dominant in this system.

Thus, it is apparent that the higher the volume fraction of a 25 wt % toluene-diluted heavy oil in water, the larger the droplets for a given energy dissipation rate. These results also confirmed that energy dissipation in a stirred tank with two phases is not the only factor that determines the droplet size. The sizes appear to depend also on the volume fraction of the dispersed phase and the flow property of the internal oil phase. The occurrence of larger sizes at the high volume fraction was more reasonably explainable by a balance between breakage and coalescence, with coalescence being more effective as the droplets are closer to each other.

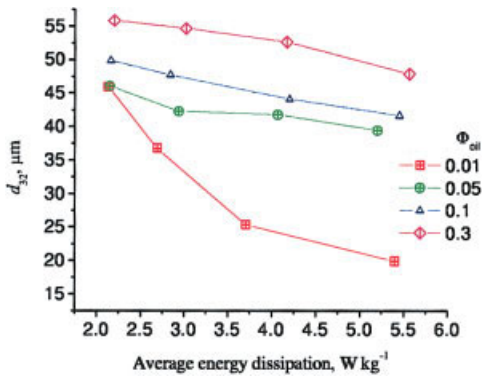


**Figure 10. Effects of average energy dissipation $\bar{\varepsilon}_T$ on the diameters $d_{32}$ of oil droplets of $\Phi_{oil}$ = 0.01, 0.05, 0.1, and 0.3 formed in model process water ($mpH_2O$) at 75 min mixing.[38]**

[Color figure can be viewed in the online issue, which is available at www.interscience.wiley.com]

### *Breakage as a first-order kinetic process for midrange oil fractions at 800 rpm*

The parallel but linear responses of $d_{32}$ vs. rpm for oil fractions 0.05 and 0.1 show more ordered breakage behavior. The kinetic first-order breakage function (Eq. 1) was fitted by least-squares regression to the experimental data $d_{32}$ vs. time for oil fractions 0.05 and 0.1 (Figures 2a and 3a). The derivation of this function was described in a previous publication,[10] where $d_{32}^{ss}$ represents the calculated steady-state size:

$$d_{32} = d_{32}^{ss} + B \exp(-k_1 t) \quad (1)$$

The kinetic constants $k_1$ with the coefficients $B$ and the calculated $d_{32}$ at steady state are tabulated in Table 2.

The results in Table 2 are in reasonable agreement with a first-order kinetic breakage process. The $R^2$ values are >96%. Breakage rate constants $k_1$ suggest that collisions resulting in breakage were close. However, the larger steady-state size at the higher oil fractions indicates that the oil fraction influences the overall average size of the droplets.

The next question to be addressed is: Do the heavy oil systems behave according to size-predictive models based on the balance of turbulent and interfacial stresses, at increased oil fractions? This topic is addressed in another paper based on this work.[38]

## Conclusions

(1) Increasing volume fractions of oil phase led to increasingly larger droplet diameters at all agitation speeds studied in turbulent mixing of 25 wt % heavy oil in toluene in model process water. The largest size droplets occurred for the highest volume fraction of oil phase. Results were consistent with published results on similar behavior that was explained as turbulence-dampening effects.

(2) The bimodal droplets size distributions for heavy oil volume fractions of 0.01 after prolonged mixing at 800 and 900 rpm were reflected as step change in average droplet sizes. The probability of a reduced collision frequency at the lower oil phase ratios favored the dominance of breakage. Breakage resulting in bimodal distribution was attributed to satellite drop formation. Lack of bimodal behavior at the higher oil volume fractions was consistent with published findings on other systems. Broadened size distributions after rest for $\Phi_{oil}$ = 0.01 mixed at 800 to 900 rpm indicated changes in the sample exposed to air, and a very slow coalescence even at high droplet packing density.

(3) Small droplets remain in a broadened size distribution. As agitation time progressed for each oil phase at volume

**Table 2. Constants and Coefficients for a First-Order Breakage Rate Function at 800 rpm**

| $\Phi_{oil}$ | $d_{32}^{ss}$ (μm) | $B$ | $k_1$ (min$^{-1}$) | $R^2$ | $\varepsilon_T$ (W kg$^{-1}$) |
|---|---|---|---|---|---|
| 0.05 | 41.67 ± 0.28 | 7.8 ± 0.5 | 0.054 | 0.97 | 4.1 |
| 0.1 | 43.9 ± 0.3 | 8.1 ± 0.6 | 0.053 | 0.96 | 4.2 |

fractions $> 0.01$, the size distributions narrowed and reached a steady state before the end of the mixing time. High electrical double-layer repulsive forces of the charged droplets would contribute to reduced coalescence after breakup.

(4) Segregation of droplet sizes vs. time curves as mixing speeds changed from 600 to 900 rpm and the widest spread at 700 rpm at oil fractions of 0.05 to 0.3 indicated transient changes in the systems with energy. Summary plots of $d_{32}$ vs. rpm after 75 min mixing, show behavior went from concave to linear to convex, as the volume fraction of oil phase increased.

(5) The oil fractions 0.05 and 0.1 followed first-order breakage in time function best at 800 rpm.

(6) At an equal energy dissipation rate the larger droplet sizes at oil fraction of 0.3 and the shapes of the curves with energy dissipation rates indicated that turbulent dampening and reduced coalescence were not the only parameters controlling droplet sizes. Droplet resistance to breakage from their elastic films appears to play a role as well. However, at an oil volume fraction of 0.3 there were indications of instability setting in as droplet number density increased.

## Acknowledgments

Financial support for this work was provided by Canada Federal Panel for Energy Research and Development and the CETC/Devon Advanced Separations Technology Laboratory. C. W. Angle thanks Dr. T. Dabros of CETC/AST and Dr. Leo Lue of UMIST for the critical reviews of the PhD dissertation and Ms. Ng for assistance while doing the experiments.

## Notation

$D_T$ = tank diameter
$D_T/3$ = off-bottom clearance position of impeller in tank
$d_{32}$ = Sauter mean diameters, $d_{32} = \Sigma_i^k n_i d_i^3 / \Sigma_i^k n_i d_i^2$
$d_{32}^{ss}$ = steady-state diameter
$d_i$ = diameter of droplet of identity $i$
$n_i$ = number of droplets of identity $i$
$H$ = liquid height
$k_1$ = kinetic constants
$B$ = coefficient
$mpH_2O$ = model process water
rpm = impeller revolutions per minute
$t$ = time

### *Greek letters*

$\bar{\varepsilon}_T$ = mean rate of energy dissipation, W kg$^{-1}$
$\Phi_{oil}$ = volume fraction of toluene-diluted heavy oil

## Literature Cited

1. Angle CW. Chemical demulsification of stable crude oil and bitumen emulsions in petroleum recovery—A review. In: Sjoblom J, ed. *Encylopedic Handbook of Emulsion Technology*. 1st Edition. New York, NY: Marcel Dekker; 2001:541-594.
2. Davies JT. *Turbulence Phenomena—An Introduction to the Eddy Transfer of Momentum, Mass, and Heat, Particularly at Interfaces*. New York, NY: Academic Press; 1972.
3. Davies JT. Drop sizes of emulsions related to turbulent energy dissipation rates. *Chem Eng Sci.* 1985;40:839-842.
4. Davies GA. Mixing and coalescence phenomena in liquid–liquid systems. In: Thornton JD, ed. *Science and Practice of Liquid–Liquid Extraction*. Oxford, UK: Clarendon Press; 1992;1:245-342.
5. Doulah MS. An effect of hold-up on drop sizes in liquid–liquid dispersions. *Ind Eng Chem Fundam.* 1975;14:137-138.
6. Chesters AK. The modelling of coalescence processes in fluid–fluid dispersions: A review of current understanding. *Trans IChemE.* 1991; 69A:259-270.
7. Abid S, Chesters AK. The drainage and rupture of partially-mobile films between colliding drops at constant approach velocity. *Int J Multiphase Flow.* 1994;20:613-629.
8. Chesters AK, Hofman G. Bubble coalescence in pure liquids. *Appl Sci Res.* 1982;38:353-361.
9. Angle CW, Hamza HA, Dabros T. Size distributions and stability of toluene diluted heavy oil emulsions. *AIChE J.* 2006;52:1257-1266.
10. Angle CW. Effects of sand fraction on toluene-diluted heavy oil in water emulsions in turbulent flow. *Can J Chem Eng.* 2004;82:722-734.
11. Angle CW. *Stability of Heavy Oil Emulsions in Turbulent Flow and Different Chemical Environments*. PhD. Thesis. Manchester, UK: University of Manchester Institute of Science and Technology; 2004:1-424.
12. Hinze JO. Fundamentals of the hydrodynamic mechanisms of splitting in dispersion processes. *AIChE J.* 1955;1:289-295.
13. Lagisetty JS, Das PK, Kumar R, Gandhi KS. Breakage of viscous and non-Newtonian drops in stirred dispersions. *Chem Eng Sci.* 1986;41: 65-72.
14. Taylor SD, Czarnecki J, Masliyah J. Disjoining pressure isotherms of water-in-bitumen emulsion films. *J Colloid Interface Sci.* 2002;252: 149-160.
15. Coulaloglou CA, Tavlarides LL. Drop size distributions and coalescence frequencies of liquid–liquid dispersions in flow vessels. *AIChE J.* 1976;22:289-297.
16. Ferworn KA. *Thermodynamics and Kinetic Modelling of Asphaltene Precipitation from Heavy Oils and Bitumens*. PhD Thesis. Calgary, Alberta, Canada: University of Calgary; 1995:1-236.
17. Kolmogorov AM. Breakup of droplets in turbulent flow. *Dokl Acad Nauk USSR.* 1949;66:825-828.
18. Kumar S, Kumar R, Gandhi KS. A multistage model for drop breakage in stirred vessels. *Chem Eng Sci.* 1992;47:971-980.
19. Desnoyer C, Masbernat O, Gourdon C. Experimental study of drop size distributions at high phase ratio in liquid–liquid dispersions. *Chem Eng Sci.* 2003;58:1353-1363.
20. Karam HJ, Bellenger JC. Deformation and breakup of liquid drops in a simple shear field. *Ind Eng Chem Fundam.* 1968;7:576-581.
21. Baldyga J, Bourne JR, Pacek AW, Amanullah A, Nienow AW. Effects of agitation and scale-up on drop size in turbulent dispersions: Allowance for intermittency. *Chem Eng Sci.* 2001;56:3377-3385.
22. Pacek AW, Man CC, Nienow AW. On the Sauter mean diameter and size distributions in turbulent liquid/liquid dispersions in a stirred vessel. *Chem Eng Sci.* 1998;53:2005-2011.
23. Angle CW, Lue L, Dabros T, Hamza HA. Viscosities of heavy oils-in-toluene and partially-deasphalted heavy oils-in-heptol in a study of asphaltenes self-interactions. *Energy Fuels.* 2005;19:2014-2020.
24. Koshy A, Das TR, Kumar R, Gandhi KS. Breakage of viscoelastic drops in turbulent stirred dispersions. *Chem Eng Sci.* 1988;43:2625-2631.
25. Walter JF, Blanch HW. Bubble break-up in gas–liquid bioreactors: Break-up in turbulent flows. *Chem Eng J.* 1986;32:B7-B17.
26. Lee JC, Tasakorn P, Belghazi A. Fundamentals of drop breakage in the formation of liquid–liquid dispersions. Proceedings of the 3rd European Conference on Mixing, The formation of liquid–liquid dispersions chemical and engineering aspects. York, UK: British Hydromechanics Research Association; 1979;157:43-57.
27. Skelland AHP, Lee JM. Agitator speeds in baffled vessels for uniform liquid–liquid dispersions. *Ind Eng Chem Process Des Dev.* 1978;17: 473-478.
28. Lee JM, Soong Y. Effects of surfactants on the liquid–liquid dispersions in agitated vessels. *Ind Eng Chem Process Des Dev.* 1985;24: 118-121.
29. Chatzi EG, Kiparissides C. Drop size distributions in high holdup fraction dispersion systems: Effect of the degree of hydrolysis of PVA stabilizer. *Chem Eng Sci.* 1994;49:5039-5052.
30. Sovova H. Breakage and coalescence of drops in a batch stirred vessel—II. Comparison of model and experiments. *Chem Eng Sci.* 1981;36:1567-1573.
31. Nambiar DKR, Kumar R, Das TR, Gandhi KS. A new model for breakage frequency of drops in turbulent stirred dispersions. *Chem Eng Sci.* 1992;47:2989-3002.
32. Kumar S, Kumar R, Gandhi KS. A new model for coalescence efficiency of drops in stirred dispersions. *Chem Eng Sci.* 1993;48:2025-2038.
33. Tsouris C, Tavlarides LL. Breakage and coalescence models for drops in turbulent dispersions. *AIChE J.* 1994;40:395-406.

34. Thomas RM. Bubble coalescence in turbulent flows. *Int J Multiphase Flow.* 1981;7:709-717.
35. Eley DD, Hey MJ, Lee MA. Rheological studies of asphaltene films adsorbed at the oil/water interface. *Colloids Surf.* 1987;24:173-182.
36. Mohammed RA, Bailey AI, Luckham PF, Taylor SE. The effect of demulsifiers on the interfacial rheology and emulsion stability of water-in-crude oil emulsions. *Colloids Surf A: Physicochem Eng Aspects.* 1994;91:129-139.
37. Dreher TM, Glass J, O'Connor AJ, Stevens GW. Effect of rheology on coalescence rates and emulsion stability. *AIChE J.* 1999;45:1182-1190.
38. Angle CW, Hamza HA. Predicting the sizes of toluene-diluted heavy oil emulsions in turbulent flow. Part 2. Hinze–Kolmogorov based model adapted for increased oil fractions and energy dissipation in a stirred tank. *Chem Eng Sci*. 2006:1-31. doi:10.1016/j.ces.2006/01/014

*Manuscript received May 11, 2005, and revision received Mar. 9, 2006.*